# GROGRAT: A NEW MODEL OF THE GLOBAL PROPAGATION AND DISSIPATION OF ATMOSPHERIC GRAVITY WAVES

Stephen D. Eckermann[1] and Crispin J. Marks[2]

[1]*Computational Physics, Inc., Suite #600, 2750 Prosperity Avenue, Fairfax, VA 22031, USA.*
[2]*National Institute of Water and Atmospheric Research, Ltd., Wellington, New Zealand.*

ABSTRACT

We describe the most recent version of the ***G***ravity-wave ***R***egional ***O***r ***G***lobal ***Ra***y ***T***racer (GROGRAT), a ray-tracing model of the propagation and amplitude evolution of gravity waves within any gridded numerical representation of the Earth's lower and/or middle atmosphere. Here we describe new features of the GROGRAT code and some recent results, including a global simulation using the CIRA-86 climatological middle atmosphere and some preliminary simulations of regional mountain-wave activity.

INTRODUCTION

The general circulation of the middle atmosphere is sensitively dependent on the global morphology of Eliassen-Palm (EP) flux divergence, which is dominated by gravity-wave dissipation in the mesosphere and equatorial stratosphere (e.g., Mengel *et al*., 1995). Yet synoptic-scale data on gravity-wave activity has only begun to emerge recently (Tsuda *et al*., 1994; Fetzer and Gille, 1994; Allen and Vincent, 1995; Eckermann *et al*., 1995). As this observational picture develops, it is important that there are parallel developments of global models of gravity-wave activity, so that our understanding of the gravity-wave data bases improves, leading to improved simulations of gravity waves, and hence of middle atmosphere circulations.

Ray-tracing models have shown promise in simulating the behavior of gravity waves within both atmospheric and oceanic environments (e.g., Dunkerton and Butchart, 1984; Schoeberl, 1985; Henyey *et al*., 1986; Eckermann, 1992). To assess the full capability of the ray-tracing method, a three-dimensional global-scale nonhydrostatic ray-tracing model of atmospheric gravity-wave propagation and activity was developed by Marks and Eckermann (1995). This model, which we now refer to as GROGRAT (version 1.0), proved useful in simulating a range of gravity-wave effects. Thus we have continued development of the GROGRAT code, and this paper reports on new features of and results from the most recent release (version 2.7) of the model.

FORMULATION AND RECENT IMPROVEMENTS

The theory and computational implementation of version 1.0 of GROGRAT were described in detail by Marks and Eckermann (1995). Briefly, gravity-wave group trajectories, wavenumber refraction and amplitude evolution are computed within a gridded numerical representation of the atmosphere by integrating a general set of ray equations. The atmosphere is assumed to vary in all three spatial dimensions. Global atmospheres are fitted with spherical harmonics, which are interconnected in the vertical with cubic spline fits of the spherical harmonic coefficients. Regional atmospheric "cubes" are fitted with cubic splines in all three spatial dimensions. The model also computes gravity-wave amplitudes along the ray path using wave-action conservation principles, and includes parameterizations of turbulent and radiative wave damping, and wave-amplitude saturation.

We have since upgraded GROGRAT to "next generation" status (version 2). The major purpose of this upgrade was to make the model fully four-dimensional, so that time variations of the background atmosphere could also be included. The ray-tracing equations were upgraded to respond appropriately to time variations of the atmosphere (Eckermann and Marks, 1996), which were fitted and interpolated using cubic splines. A host of other upgrades have also been made. The major scientific ones are:

- provision for a background vertical velocity field, with the gravity-wave ray-tracing equations generalized accordingly (e.g., Jones, 1969);
- provision for model atmospheres which are gridded on pressure or log-pressure surfaces. These atmospheres are now regridded internally by GROGRAT onto a regular geometrical height grid;
- provision for both "forwards" (in time) and "backwards" ray-tracing experiments;
- incorporation of the scale-dependent $CO_2$ and $O_3$ radiative-damping parameterizations of Zhu (1993), which extend from the ground to 120 km;
- reduction of the climatological eddy diffusivity profile in the model by a factor of 3, based on recent reappraisals of observational data sets (Hocking, 1996);

Development of GROGRAT continues, and further upgrades are likely. The status of the model can be monitored by accessing the GROGRAT homepage at http://uap-www.nrl.navy.mil/dynamics/html/grograt.html.

RECENT RESULTS

Global Gravity-Wave Propagation Through the 1986 COSPAR International Reference Atmosphere (CIRA-86)

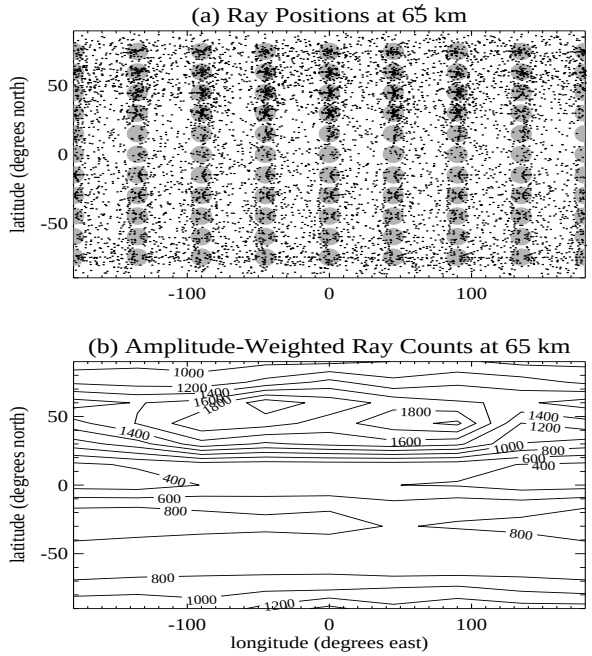


Fig. 1. (a): locations of rays which propagate to $z$ = 65 km. Circles mark launch locations at $z_0$ = 5 km; (b) number of rays (scaled by their final horizontal velocity amplitude) which reach $z$ = 65 km.

In the following GROGRAT simulation, each ray was assigned an initial horizontal velocity amplitude $u'$ = 0.1 m $s^{-1}$, and one of 7 horizontal wavelengths $\lambda_h$, 5 ground-based horizontal phase speeds $c_h$ (0-40 m $s^{-1}$), and 8 equispaced propagation azimuths $\phi$ (0-360$^o$). This yielded 280 different rays, which were launched at $z_0$ = 5 km from 88 different locations over the globe (shown with shaded circles in panel *a*), giving 24640 rays in all. Figure 1 shows results for rays reaching $z$ = 65 km using global winds and temperatures derived from the CIRA-86 fields for January (Marks, 1989), which GROGRAT fitted with spherical harmonics truncated at order 8 both zonally and meridionally. The wind fields near the equator are inaccurate, so the equatorial results should be discounted. These simulations also did not permit cross-polar propagation, and so wave transmission at the poles may be underestimated.

The combined results in Figure 1b show interesting similarities with gravity-wave data for January-February 1979 inferred from global temperature measurements from LIMS (Figures 19-20 of Fetzer and Gille (1994)): specifically, wave amplitudes in the Northern Hemisphere are larger and more zonally asymmetric than those in the Southern Hemisphere. The zonal asymmetries, which arise from the filtering effects of stratospheric Rossby waves (Dunkerton and Butchart, 1984; Schoeberl, 1985; Marks and Eckermann, 1995), differ in form from those reported by Fetzer and Gille (1994). This may be due in part to differences between the climatological CIRA winds and the time-varying flow patterns during the warming events of January-February 1979 (see, e.g., Dunkerton and Butchart, 1984; Figures 25-26 of Fetzer and Gille, 1994). The simulated differences in wave amplitudes between the summer and winter hemispheres are consistent with the theory of Eckermann (1995).

Figure 2 shows histograms of $\lambda_h$, $c_h$, and $\phi$ for rays reaching 65 km. The peaks in each panel show the various values that were assigned at $z_0$ = 5 km. We note preferential transmission of $\lambda_h$ values of ~50-100 km into the mesosphere, but no preferential removal of $c_h$ values globally. Remarkably, however, no $c_h$ = 0 waves propagate to 65 km anywhere in the Southern Hemisphere. More large-$c_h$ waves reach 65 km in the Southern (summer) Hemisphere than in the Northern Hemisphere, which is consistent with the need for nonzero phase-speed waves in models of the summer mesospheric circulation (e.g., Jackson, 1993). As in the earlier two-dimensional

hydrostatic simulations (Eckermann, 1992), westward (eastward) $\phi$'s dominate in the summer (winter) hemisphere due to filtering by the underlying stratospheric flow, and meridionally-aligned waves are efficiently transmitted into the mesosphere in both hemispheres.

Mountain Wave "Forecasts"

Figure 1a shows that waves which reach 65 km in the Northern Hemisphere remain "clumped" above their launch spots, due to the strong transmission of stationary ($c_h$ = 0) waves. Thus, geographical "hot spots" in stationary mountain-wave (MW) activity can be transmitted quasi-vertically to produce further zonal asymmetries in mesospheric wave activity in the Northern Hemisphere in January (e.g., Bacmeister, 1993), possibly accounting for further differences between Figure 1b and the data of Fetzer and Gille (1994).

To study this further, GROGRAT has been used with a ridge database and an extended MW-forcing model (based on the model of Bacmeister *et al.* (1994)) which gives an inital $z_0$, $u'$, $\lambda_h$ and $\phi$ for each forced wave. Figure 3 shows predicted MW ray paths over New Zealand for the 24th and 25th October, 1994. Winds and temperatures came from six-hourly GASP analyses (Seaman *et al.*, 1995), and total wind speed is contoured at 7 km (top row) and at 172°E (bottom row). We note large changes in predicted MW behavior on each day: early on the 24th, there is strong production on the South Island which propagates well into the stratosphere, whereas late on the 25th there is more MW production on the North Island, and this activity is confined to the troposphere. Stars on the ray path indicate likely saturation and turbulence production. While these results are preliminary, comparisons with stratospheric aircraft data have been encouraging so far, so that this model may ultimately provide computationally-inexpensive MW-turbulence forecasts to aid flight planning, for example (Bacmeister *et al.*, 1994).

SUMMARY

The examples discussed here represent only a selection of problems to which GROGRAT can be applied. For example, GROGRAT has also proved useful as a purely theoretical tool, providing important insights into gravity-wave tidal interactions in the mesosphere (Eckermann and Marks, 1996; see also Zhong *et al.*, 1995) and interactions among a random spectrum of atmospheric gravity waves (Eckermann, 1996). It provides a general yet flexible means of simulating gravity-wave propagation and amplitude variability within arbitrary atmospheric environments. Further enhancements of and experiments with GROGRAT are either planned or in progress, and

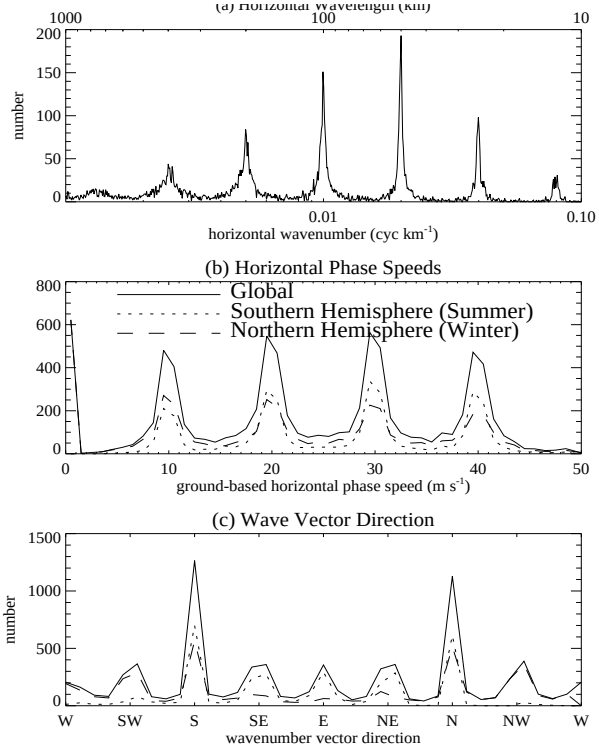


Fig. 2. Histograms of ray parameters at 65 km: (a) horizontal wavelengths; (b) ground-based horizontal phase speeds; (c) horizontal wave-vector directions. The binning interval is linear in (b)-(c), and logarithmic (in wavenumber) in (a) .

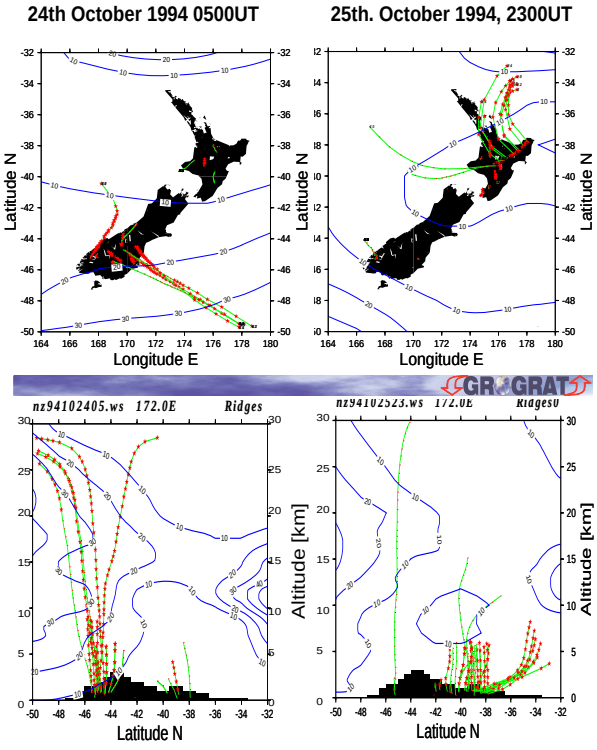


Fig. 3. Simulated mountain-wave production and ray paths (starred curves) over New Zealand on 24th October (0500 GMT) and 25th October (2300 GMT), 1994. Contours are total wind speed (in m $s^{-1}$). Land and orographic features are silhouetted.

will be reported upon in due course.

REFERENCES


Allen, S. J., and R. A. Vincent, Gravity-wave activity in the lower atmosphere: Seasonal and latitudinal variations, *J. Geophys. Res*., **100**, 1327 (1995).

Bacmeister, J. T., Mountain-wave drag in the stratosphere and mesosphere inferred from observed winds and a simple mountain-wave parameterization scheme, *J. Atmos. Sci*., **50**, 377 (1993).

Bacmeister, J. T., P. A. Newman, B. L. Gary, and K. R. Chan, An algorithm for forecasting mountain wave-related turbulence in the stratosphere, *Wea. Forecasting*, **9**, 241-253 (1994).

Dunkerton, T. J., and N. Butchart, Propagation and selective transmission of internal gravity waves in a sudden warming, *J. Atmos. Sci*., **41**, 1443 (1984).

Eckermann, S. D., Ray-tracing simulation of the global propagation of inertia gravity waves through the zonally-averaged middle atmosphere, *J. Geophys. Res*., **97**, 15,849 (1992).

Eckermann, S. D., On the observed morphology of gravity-wave and equatorial-wave variance in the stratosphere, *J. Atmos. Terr. Phys*., **57**, 105 (1995).

Eckermann, S. D., Influence of wave propagation on the Doppler-spreading of atmospheric gravity waves, *J. Atmos. Sci*., (submitted) (1996).

Eckermann, S. D., and C. J. Marks, An idealized ray model of gravity wave-tidal interactions, *J. Geophys. Res*., (in press) (1996).

Eckermann, S. D., I. Hirota, and W. K. Hocking, Gravity wave and equatorial wave morphology of the stratosphere derived from long-term rocket soundings, *Q. J. R.. Meteorol. Soc*., **121**, 149 (1995).

Fetzer, E. J., and J. C. Gille, Gravity wave variance in LIMS temperatures. Part I: Variability and comparison with background winds, *J. Atmos. Sci*., **51**, 2461 (1994).

Henyey, F. S., J. Wright, and S. M. Flatté, Energy and action flow through the internal wave field: An eikonal approach, *J. Geophys. Res*., **91**, 8487 (1986).

Hocking, W. K., An assessment of the capabilities and limitations of radars in measurements of upper atmosphere turbulence, *Adv. Space Res*., **17**, (11)37 (1996).

Jackson, D. R., Sensitivity of the Extended UGAMP General Circulation Model to the specification of gravity-wave phase speeds, *Q. J. R. Meteorol. Soc*., **119**, 457 (1993).

Jones, W. L., Ray tracing for internal gravity waves, *J. Geophys. Res*., **74**, 2028 (1969).

Marks, C. J., Some features of the climatology of the middle atmosphere revealed by Nimbus 5 and 6, *J. Atmos. Sci*., **46**, 2485 (1989).

Marks, C. J., and S. D. Eckermann, A three-dimensional nonhydrostatic ray-tracing model for gravity waves: Formulation and preliminary results for the middle atmosphere, *J. Atmos. Sci*., **52**, 1949 (1995).

Mengel, J. H., H. G. Mayr, K. L. Chan, C. O. Hines, C. A. Reddy, N. F. Arnold, and H. S. Porter, Equatorial oscillations in the middle atmosphere generated by small scale gravity waves, Geophys. Res. Lett., **22**, 3027 (1995).

Schoeberl, M. R., A ray tracing model of gravity wave propagation and breakdown in the middle atmosphere, *J. Geophys. Res*., **90**, 7999 (1985).

Seaman, R., W. Bourke, P. Steinle, T. Hart, G. Embury, M. Naughton, and L. Rikus, Evolution of the Bureau of Meteorology's global assimilation and prediction system. Part I: Analysis and initialization, *Aust. Met. Mag*., **44**, 1-18 (1995).

Tsuda, T., Y. Murayama, T. Nakamura, R. A. Vincent, A. H. Manson, C. E. Meek, and R. L. Wilson, Variations of the gravity-wave characteristics with height, season and latitude revealed by comparative observations, *J. Atmos. Terr. Phys*., **56**, 555 (1994).

Zhong, L., L. J. Somnor, A. H. Manson, and C. E. Meek, The influence of time-dependent wind on gravity-wave propagation in the middle atmosphere, *Ann Geophysicae*, **13**, 375 (1995).

Zhu, X., Radiative damping revisited: Parameterization of damping rate in the middle atmosphere, *J. Atmos. Sci*., **50**, 3008 (1993).